JOURNAL OF CATALYSIS 140, 353–369 (1993)

Influence of the Carrier on the Interaction of H_2 and CO with Supported Rh

THEOPHILOS IOANNIDES AND XENOPHON VERYKIOS

Institute of Chemical Engineering and High Temperature Chemical Processes, Department of Chemical Engineering, University of Patras, GR-26110 Patras, Greece

Received June 5, 1992; revised October 7, 1992

The influence of the carrier (SiO_2, Al_2O_3, and TiO_2) on the interaction of supported Rh with H_2 and CO and on kinetic parameters in CO hydrogenation is investigated employing transient and steady-state techniques. TPD of H_2 revealed two modes of adsorption on Rh/Al_2O_3 and Rh/TiO_2, one of which is activated. This was not observed over Rh/SiO_2. TPD spectra obtained following CO adsorption reveal significant differences, depending on the carrier. Three major states of desorbing CO were detected, one of which desorbs as CO_2 accompanied by H_2 evolution. In Rh/SiO_2 and Rh/Al_2O_3 the weakly adsorbed CO exhibits peak maximum temperatures in the range 90–100°C, while for the strongly adsorbed CO these are in the range 263–270°C in Rh/SiO_2 and 210–245°C in Rh/Al_2O_3. In both cases, the CO_2 peak maximum appears in the range 340–355°C. The activity of the catalysts toward CO decomposition was found to decrease in the order: $Rh/TiO_2 \gg Rh/Al_2O_3 > Rh/SiO_2$. This observation has been attributed to the creation of new adsorption sites at the Rh–TiO_2 interface and carrier participation in the process of CO decomposition. The reactivity of adsorbed CO toward hydrogenation, as investigated by TPR experiments, was found to follow the same order as that for CO decomposition. The Rh/TiO_2 catalyst was found to be 15–20 times more active in steady-state CO hydrogenation, as compared to Rh/SiO_2 and Rh/Al_2O_3, and to exhibit lower activation energies for methanation and water–gas shift reactions.

INTRODUCTION

The adsorption of H_2 and CO on Group VIII metal surfaces has been the subject of extensive research efforts, since these metals are active catalysts for CO hydrogenation and other CO transformation reactions. It has been shown by many investigators (*1–5*) that kinetic parameters are frequently influenced by the nature of the carrier employed to disperse the metallic phase. The mechanism of the influence of the carrier on chemisorptive and kinetic parameters is not always well understood.

The adsorption of H_2 on Rh(111) surfaces was investigated by Yates *et al.* (*6*) with TPD techniques. A single H_2 desorption peak was detected, whose maximum was found to vary between 117 and 2°C with increasing surface coverage. Similarly, a single desorption peak, varying between 235 and 165°C with increasing surface coverage, was observed by Efstathiou and Bennett (*7*) over a 5.2% Rh/Al_2O_3 catalyst. On the other hand, Bertucco and Bennett (*8*) detected two H_2 desorption peaks from a 10% Rh/SiO_2 catalyst, a major one at 162–167°C and a smaller one at 42°C. Apple *et al.* (*9*) detected three desorption peaks from Rh/TiO_2 following a 4-h H_2 adsorption at 300°C, with peak maximum temperatures at 80, 240, and 540°C. These peaks were attributed to H_2 desorption from Rh. Hydrogen desorption from Rh/TiO_2 was also investigated by Stockwell *et al.* (*10*), who observed a major desorption peak at approximately 107°C and a broad one between 280 and 430°C, which was attributed to H_2 originating from the carrier, following a spillover process. The adsorption of H_2 on Rh has been found to be a nonactivated process (*6–8*), while the heat of adsorption at low surface coverages was found to be in the neighborhood of 20 kcal/mol (*7, 8*) and to decrease significantly with increasing surface coverage.

0021-9517/93 $5.00

CO adsorbs molecularly on Group VIII metal surfaces (*11*, *12*) in contrast to dissociative adsorption on other transition metal surfaces. It can adsorb in three modes, linear, bridged, and the dicarbonyl mode. CO desorbs from Rh(111) or polycrystalline Rh surfaces following first-order kinetics (*12*). The TPD spectrum consists of a single peak at 210–260°C (*13*, *14*), while a shoulder peak which often appears to the left of the major peak is attributed to CO adsorbed in the bridged mode. CO dissociation is generally considered to be negligible under ultra-high vacuum conditions. Similar features have also been observed in TPD spectra over a Rh/α-Al_2O_3 {0001} catalyst, under ultra-high vacuum conditions (*15*).

Significantly different TPD spectra are observed over Rh dispersed on high-surface-area carriers, in which case both CO and CO_2 are detected to desorb. Over Rh/Al_2O_3, Efstathiou (*16*) observed a single CO peak at approximately 190°C and two CO_2 peaks, a major one at 320 and a minor one at 90°C. The low-temperature CO_2 peak was not considered to originate from CO decomposition (Boudouard reaction) but from the interaction of CO with hydroxyl groups of the carrier. TPD spectra over Rh/Al_2O_3 have also been reported by Oh and Eickel (*17*), who detected CO desorbing at 230–240°C, and by Erdöhelyi and Solymosi (*2*), who report a CO peak at 200°C and two CO_2 peaks at 200 and 315°C. Similar features concerning CO desorption were observed by the same authors over Rh/SiO_2 and Rh/TiO_2 catalysts, however, the second CO_2 peak was not observed over Rh/SiO_2.

CO hydrogenation over Rh/Al_2O_3 was investigated using transient isotopic techniques by Efstathiou and Bennett (*18*), who observed that under reaction conditions the largest fraction of the metallic surface is occupied by CO and a smaller fraction by active and inactive carbon. Hydrogen coverage was observed to be very small. Erdöhelyi and Solymosi (*2*) report that CO decomposition activity on Rh is affected by the nature of the carrier, decreasing in the order: $TiO_2 > Al_2O_3 > SiO_2 > MgO$. An identical order concerning the rate constants of CO decomposition and hydrogenation of CH_x species is reported by Mori *et al.* (*3*). The influence of the support on CO hydrogenation over supported Rh was also investigated by Katzer *et al.* (*19*) and Solymosi *et al.* (*20*). The former authors observed similar activation energy for CH_4 formation over Rh/SiO_2, Al_2O_3, TiO_2, in the range of 32 kcal/mol, while the latter authors observed the lowest activation energy over Rh/TiO_2 (18.3 kcal/mol) and the highest over Rh/Al_2O_3 (24.0 kcal/mol). In both cases the order of activity was found to be: Rh/TiO_2 > Rh/Al_2O_3 > Rh/SiO_2. In terms of selectivity, there is a general agreement that Rh/SiO_2 produces mainly methane, while Rh/TiO_2 produces the largest amount of higher hydrocarbons. The reaction rate constants have been found to depend inversely on metal dispersion (*3*, *21*). The influence of temperature of reduction, primarily as related to the SMSI phenomenon of Rh/TiO_2, has been investigated (*22–24*).

The influence of the carrier on the interaction of H_2 and CO with supported Rh crystallites, as revealed by TPD and TPR studies, and on kinetic parameters in CO hydrogenation under steady-state conditions, is discussed in the present communication.

EXPERIMENTAL

(*a*) *Catalyst Preparation and Characterization*

The carriers employed in the preparation of Rh catalysts are SiO_2 (Alltech Associates), γ-Al_2O_3 (Akzo Chemicals), and TiO_2 (Degussa, P-25), with surface areas of 300, 100, and 50 m^2/g, respectively. Catalysts were prepared by the method of incipient wetness impregnation, using $RhCl_3 \cdot 3H_2O$ as the precursor compound for the metal: 60–120 mg of $RhCl_3 \cdot 3H_2O$ were dissolved in 10 ml of distilled water at a temperature of 25°C, then 5–10 g of the carrier were added to the solution under continuous stirring at the same temperature. When the water evaporated, the solid material was dried

in an oven at 110°C for 24 h. It was subsequently crashed and sieved in the particle range 0.06–0.25 mm.

The crashed and sieved material was placed in a stainless steel tube of 1 cm diameter and it was heated to 200°C at a rate of 5°C/min under N_2 flow (50 cm^3/min). It was maintained under these conditions for 1 h to desorb most of the H_2O and the flow was then switched to H_2 (50 cm^3/min) to reduce the precursor compound to Rh^0. It was maintained under H_2 flow at 200°C for 1 h and for 1 more hour at 250°C. The catalyst was then slowly cooled to room temperature under N_2 flow and it was stored in airtight vials until further use. The metal content of the catalysts was invariably 0.5 wt%.

The metal dispersion of the catalysts was determined by static equilibrium adsorption of H_2 at room temperature. A constant volume high-vacuum apparatus (Micromeritics, Accusorb 2100 E) was used for this purpose. A small quantity of the catalyst (0.5 g) was placed under dynamic vacuum at 200°C for 2 h so as to desorb gases adsorbed on the catalyst surface. The sample was then exposed to H_2 (200 Torr) for 1 h at 250°C and subsequently placed under dynamic vacuum for approximately 10 h. It was then cooled to 25°C, at which temperature hydrogen adsorption isotherms were obtained. For each measurement, equilibrium was assumed when the rate of pressure drop was less than 10^{-3} Torr/min. This normally required 1–5 h. The adsorption isotherm was obtained in the H_2 pressure range 10–300 Torr. The quantity of H_2 adsorbed at monolayer coverage was estimated by extrapolation of the linear portion of the isotherms to zero pressure, which is a standard procedure. The unmetallized supports were found not to adsorb measurable quantities of H_2 under these conditions.

(b) TPD and TPR Experiments

The TPD apparatus consists of a flow measuring and switching system, a heated quartz tube in which the catalyst is placed, and the analysis system. The flow system is composed of high precision rotameters and needle valves, 3-, 4-, and 6-way valves and switching valves. Gases can be introduced to the TPD cell in either the continuous flow mode or the pulse mode. Each pulse is 0.05 cm^3 (STP) of gas. The TPD cell is a quartz tube of 0.6 cm diameter and 15 cm length. A section at the center of the tube is expanded to 1.2 cm diameter, in which the catalyst sample, approximately 0.25 g, is placed. A $\frac{1}{16}''$ thermocouple well runs through the center of the cell, and a thermocouple is used to determine the temperature at the catalyst bed. The TPD cell is placed in a cylindrical furnace of 2.4 cm diameter which is controlled by a linear temperature programmer (Omega, CN 2010). The heating rate applied in the current study was 23°C/min.

The outlet of the cell is connected to a quadrupole mass spectrometer (Sensorlab 200D-VG Quadrupoles) via a heated silica capillary tube of 2 m length with a fast response at 1 atm sampling pressure. The mass spectrometer is connected to a personal computer for instrument control, data acquisition and analysis.

The gases used were supplied by L'Air Liquide and were of 99.995% purity. He was further purified by passing it through a heated metallic zirconium trap (Supelco Inc.), CO and O_2 through molecular sieve 5A traps, and H_2 through an Oxysorb and a molecular sieve 5A trap.

Prior to any experiments it was determined that the TPD cell or the tubing were not active in the adsorption of H_2 and CO and did not contribute to the mass spectrometer signal. Adsorption on unmetallized carriers was also investigated. The procedure for each experiment was the following: The catalyst, 0.25 g, was placed in the TPD cell, supported by quartz wool, and heated to 200°C in H_2 flow for 1 h. It was then cooled in He flow. When the temperature reached 25°C the adsorbing gas, H_2 or CO, was introduced either in the form of continuous flow (30 cm^3/min) for 15 min or in the pulse mode. In the latter case, the

volume of the pulse was 0.05 cm^3 and 5–10 pulses were introduced in each case. The flow was switched to He and the lines were cleaned for 3 min. Temperature programming was then initiated and the TPD spectra were obtained. For high-temperature adsorption of H_2, the catalyst was heated under He flow to the desired temperature, then the flow was switched to H_2 for 15 min and the catalyst was cooled to room temperature under H_2 flow. At the end of each experiment the catalyst was exposed to O_2 at 450°C for 5 min to burn off any carbon deposited, followed by H_2 reduction. This cycle was found to give very reproducible TPD and TPR results.

The design of TPD experiments and the selection of experimental parameters was done in such a way as to minimize mass transport effects as well as imperfect mixing in the TPD cell. The criteria proposed by Demmin and Gorte (*25*) were used for this purpose. The criteria concerning convective lag and diffusive lag are satisfied since the parameter values achieved in the present study are 5×10^{-4} and 3×10^{-5}, respectively, while the proposed criteria require values of less than 0.01 in both cases. Concerning particle concentration gradients and bed concentration gradients, parameter values of 0.1 and 0.3 are estimated, which are comparable to the proposed values of less than 0.05 and 0.1, respectively. It has been shown, however, that for particle concentration gradients a more realistic parameter value would be less than 1.0 (*26*), while for bed concentration gradients it has been demonstrated that for $Pe_L < 1$ deviations from the CSTR behavior are negligible (*27*).

Readsorption effects can also influence TPD spectra. It has been shown that elimination of readsorption effects in carrier gas TPD experiments over powdered catalysts, in most cases, requires experimental conditions which are not easily achievable (*26, 27*). In the present study, experimental parameters (mass of catalyst and carrier gas flow rate) were selected so as to reduce, to the extent possible, readsorption effects, within the detectability limits of the mass spectrometer. Readsorption effects are expected to be similar in the catalysts employed in the present study since their structure is not significantly different.

(*c*) *Steady-state Kinetic Measurements*

The apparatus employed for measurements of kinetic parameters in CO hydrogenation consists of a flow measuring and control system, a tubular reactor and an on-line analytical system. Feed flow rates were measured and controlled by thermal mass flow meters (MKS Instruments). The reactor is a 1-cm-I.D. stainless steel U-shaped tube, immersed in a constant temperature fluidized sand bath (Techne SBL-2D) for attainment of isothermal conditions. One of the legs of the reactor was filled with α-Al_2O_3 pellets and was used to preheat the feed mixture. The catalyst bed was placed in the other leg of the reactor, through which a $\frac{1}{8}''$ thermocouple well run along its length. The catalyst was in the form of particles of diameter between 0.125 and 0.250 mm. This size of catalyst particles was found experimentally not to offer any measurable intraparticle resistance in the transport of mass and heat. Temperature along the length of the catalyst bed was found to be constant within ±1°C.

Analysis of the feed and of the reaction mixtures was achieved by a gas chromatograph connected on-line to the reactor apparatus via a gas sampling valve. Two chromatographic columns were used for the separation of gas mixtures. A Carbosieve S-II 100/120 column was used to separate H_2, N_2, CO, CH_4, and CO_2, and it was connected to the TC detector. A Porapak QS 80/100 column was used to separate the hydrocarbons and it was connected to the FI detector.

In all cases the reactor was operated in the differential mode, with CO conversions less than 5%. The CO/H_2 reaction was investigated in the temperature range of 170 to 250°C. The feed consisted of 24% H_2, 8%

CO, and 68% N_2 (H_2/CO=3) on a molar basis. Rate measurements were obtained after the system had reached steady state, which normally required 1 to 2 h. After each measurement under a particular set of conditions the catalyst was exposed to H_2 flow for 30 min at 250°C.

RESULTS AND DISCUSSION

The supported Rh catalyst employed in the present investigation were characterized in terms of their degree of dispersion by selective equilibrium H_2 adsorption at room temperature. The volume of H_2 adsorbed at monolayer coverage was used to estimate the H/Rh ratio (atoms of hydrogen adsorbed per Rh atom in the catalyst) assuming dissociative adsorption and 1-to-1 stoichiometry. The H/Rh ratios thus estimated were found to be 1.29 for Rh/SiO_2, 1.0 for Rh/Al_2O_3, and 0.70 for Rh/TiO_2, indicating that all catalysts had a very high metal dispersion. The surface-mean diameter of the supported Rh crystallites, assuming that they are semispherical, is estimated to be between 10 and 15 Å.

(*a*) *The Interaction of H_2 with Rh/Al_2O_3, SiO_2, and TiO_2*

TPD spectra of H_2 adsorbed on 0.5% Rh/SiO_2, Al_2O_3, and TiO_2 catalysts at temperatures of 25, 120, and 190°C were obtained following the procedures described earlier. Identical experiments were also carried out with unmetallized carriers from which no H_2 desorption was observed under any conditions. TPD spectra obtained with the 0.5% Rh/SiO_2 catalyst after H_2 adsorption at three temperatures are shown in Fig. 1A. The spectra consist of a major peak at 75°C which is shifted to approximately 103°C when adsorption takes place at 190°C. Two minor shoulder peaks may be distinguished to the right of the major peak, at approximately 110 and 200–250°C. Bertucco and Bennett (*8*) observed a single desorption peak at 175°C from a 10% Rh/SiO_2 catalyst, under a heating rate of 0.6°C/s, which is considerably higher than that employed in the present study (0.38°C/s). It is well known that desorption peak temperature is shifted to higher values with increasing heating rate (*28, 29*). Thus, the results of this study are in qualitative agreement with those of Bertucco and Bennett (*8*), especially if the fact that the dispersion of the two catalysts was widely different (0.35 versus 1) is taken into account.

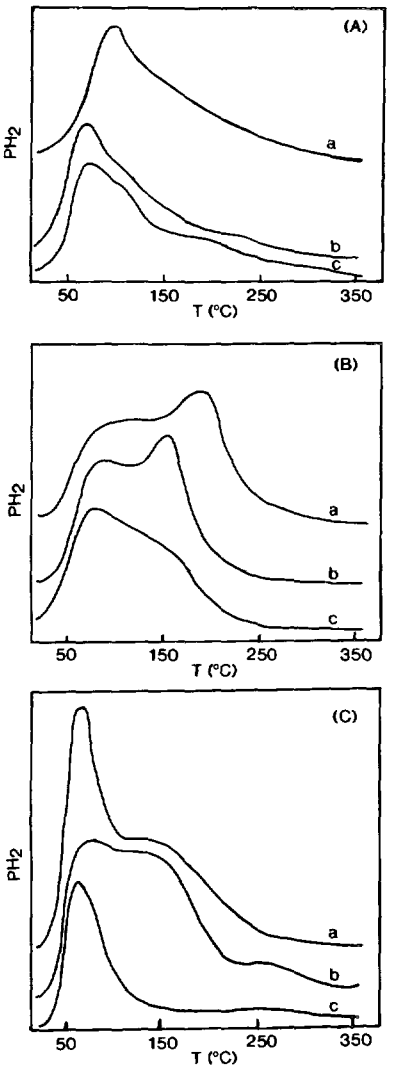

FIG. 1. TPD of H_2 from 0.5% Rh/SiO_2 (A), 0.5% Rh/Al_2O_3 (B), and 0.5% Rh/TiO_2 (C), following H_2 adsorption at 190°C (a), 120°C (b), and 25°C (c).

Corresponding spectra obtained over the

0.5% Rh/Al_2O_3 catalyst are shown in Fig. 1B, in which two desorption peaks are evident. One has a peak maximum at 90°C and is not significantly shifted with adsorption temperature. The second peak increases in intensity with increasing temperature of adsorption, while its maximum is shifted from approximately 160 to 195°C. Efstathiou and Bennett (*7*) report a single peak at 165–235°C depending on surface coverages. Their catalyst, however, had significantly lower Rh dispersion than that of the catalyst employed in the present study (0.12 versus 1.0).

TPD spectra of H_2 desorbing from the Rh/TiO_2 catalyst are shown in Fig. 1C. The low-temperature adsorption spectrum consists of a single peak at 70–80°C. However, at the higher adsorption temperatures a second peak appears at approximately 160°C. A very small peak is also observed in the neighborhood of 250–300°C. The quantity of H_2 desorbed increases significantly with increasing temperature of adsorption, indicating that H_2 adsorption on Rh/TiO_2 is an activated process. The peaks at 80 and 160°C are in relatively good agreement with those observed by Apple *et al.* (*9*) at 80 and 240°C, after H_2 adsorption at 300°C for 4 h. Under these conditions they also observed a third peak at 540°C which they attributed to H_2 spillover. Stockwell *et al.* (*10*) report a single peak at 107°C which could correspond to the 80°C peak observed in the present study.

A common feature of Rh dispersed on Al_2O_3 and TiO_2 carriers is the appearance of two peaks of desorbed H_2, which could be viewed to correspond to two modes of adsorbed hydrogen with different adsorption bonds. The TPD spectrum over Rh(111) crystals exhibits a single peak only, which may correspond to the low-temperature peak (70–100°C) observed in the Rh/SiO_2, Al_2O_3, and TiO_2 catalysts. The high-temperature peak (160–190°C) which corresponds to strongly adsorbed H_2 and possibly to activated adsorption could be due to the creation of new adsorption sites on the surface of the small Rh crystallites, which is expected to have more defects than the Rh(111) surface. It is also conceivable that the new adsorption sites are created at the metal–support interface. The concentration of these sites would be expected to increase with increased dispersion of the metal. This could be the reason why the second desorption peak has not been observed over catalysts with low Rh dispersion.

Peak temperatures of desorption are shown in Table 1 for the three catalysts investigated and the three H_2 adsorption temperatures. When the adsorption takes place at 25°C, the peak temperature does not seem to be influenced by the carrier. However, a tendency to shift peak temperatures toward higher values is observed at higher adsorption temperatures. This shift cannot be explained assuming that the surface coverage increases at higher adsorption temperatures, since the exact opposite behavior is expected in that case, i.e., shift of the peaks toward lower temperatures, as expected for second-order desorption with or without readsorption phenomena (*27*). Thus, this shift toward higher temperatures of desorption must be attributed to stronger Rh–H adsorption bonds when H_2 interacts with Rh surfaces at elevated temperature. It is also apparent that the second H_2 desorption peak appears only when adsorption has taken place at high temperatures. This peak corresponds to strongly adsorbed

TABLE 1

Peak Temperatures of Hydrogen Desorption from Supported Rh Catalysts

Catalyst Rh/	T_M (°C)		
	T_a = 25°C	= 120°C	= 190°C
SiO_2	75	75	103
Al_2O_3	80	87, 159	100, 192
TiO_2	71	80, 155	81, 160

Note. T_a is adsorption temperature; T_M is peak temperature.

TABLE 2

Quantity of H_2 Desorbed from Rh/SiO_2, Al_2O_3, and TiO_2 Catalysts after Adsorption at Different Temperatures

Catalyst Rh/	Volume of H_2 desorbed (cm^3/g)			Volume of H_2 adsorbed at equilibrium (25°C) (cm^3/g)
	T_a = 25°C	= 120°C	= 190°C	
SiO_2	0.44	0.46	0.54	0.70
Al_2O_3	0.42	0.51	0.55	0.54
TiO_2	0.15	0.28	0.36	0.28

hydrogen whose adsorption process is an activated one.

The quantity of H_2 desorbing from the 0.5% Rh catalysts is shown in Table 2, along with the quantity of H_2 found to adsorb on the same catalysts in static equilibrium chemisorption experiments at 25°C. In the Rh/Al_2O_3 and Rh/SiO_2 catalysts the quantity of H_2 desorbing is weakly affected by the temperature of adsorption, indicating that the process over these catalysts is only slightly activated, in agreement with results of other investigators (*7, 8*). In the Rh/TiO_2 catalyst, however, the quantity of desorbing H_2 increases significantly with increasing adsorption temperature, which might indicate that over this catalyst the H_2 adsorption process is an activated one. Activated H_2 chemisorption on supported metal catalysts has also been reported by other investigators (*30*). In addition to creation of new, high-energy adsorption sites on the small Rh crystallites, the phenomenon has also been attributed to the presence of surface contaminants or to decoration of the metal with oxide species originating from the support. In the present investigation the decoration effect can be rejected since the temperature of H_2 adsorption was always less than 200°C. To test whether surface contamination, primarily Cl from the metal precursor compound, contributes to H_2 adsorption at high temperature, the Rh/Al_2O_3 catalyst was reduced at 450°C, instead of the usual 200/250°C temperature, and H_2 TPD experiments were conducted following H_2 adsorption at 25, 120, and 190°C. The TPD spectra which were obtained with this catalyst were identical to the spectra obtained with the same catalyst reduced at the lower temperature. This result indicates that surface contamination is not a probable cause of the enhancement of H_2 adsorption of the Rh/TiO_2 catalyst at elevated temperatures. Thus, the most plausible causes are those stated earlier, defect sites on surfaces of small Rh crystallites or creation of new adsorption sites at the metal–support interface. The quantity of H_2 observed to desorb after adsorption at 25°C is smaller than the quantity of H_2 adsorbed at equilibrium at the same temperature. This could be due to either of two reasons: The static chemisorption measurements are equilibrium ones and have been obtained after adsorption times which exceed 10 h. On the other hand, the adsorption prior to TPD takes place under H_2 flow for only 0.5 h, time which might not be sufficient to reach equilibrium. A second reason might be that a portion of adsorbed H_2 desorbs prior to initiation of the TPD experiment, while the sample is flushed with He for 3 to 5 min to remove gas phase H_2 and to clean the lines.

This reasoning, combined with the observation that H_2 seems to be adsorbed stronger at higher adsorption temperatures might explain the observed increase of the amount of H_2 adsorbed over the Rh/TiO_2 catalyst with increasing temperature. Thus, a smaller fraction of the H_2 adsorbed at higher temperatures desorbs prior to initiation of the TPD experiment. A study of H_2 adsorption on Rh(111) has shown that adsorption and desorption proceed via an intermediate step during which a precursor state of adsorbed hydrogen is formed (*6*). If the same applies in the case of the supported Rh crystallites, then it can be assumed that the two forms of adsorbed hydrogen originate in this precursor state and the transfer from the precursor state to the strongly adsorbed state is an activated pro-

cess. For this reason, the strongly adsorbed state appears only at high temperatures.

(b) The Interaction of CO with Rh/SiO_2, Al_2O_3, and TiO_2

TPD spectra of CO over the Rh/SiO_2, Al_2O_3, and TiO_2 catalysts were obtained after CO adsorption at room temperature. The molecules detected to desorb were CO, CO_2, H_2 and CH_4. The adsorption of CO was also investigated on the unmetalized carriers. Over SiO_2, only traces of CO_2 were observed at temperatures higher than 450°C, after CO adsorption at 25°C for 15 min. The spectrum obtained over Al_2O_3 consisted of CO_2 only, in the temperature range 200–300°C. The quantity of CO_2 desorbed was found to be approximately 0.05 cm^3/g. CO_2 was also the only species observed to desorb after 15 min exposure of TiO_2 to CO at 25°C. CO_2 was observed to desorb in the temperature range of 50 to 200°C with a peak at 80°C, and its quantity was approximately 0.03 cm^3/g. These quantities of CO_2 correspond to 4–5% of quantities detected from the corresponding Rh-supported catalysts. The CO_2 in the TPD spectra of the Al_2O_3 and TiO_2 carriers probably originates from either the oxidation of CO by some oxidizing centers on the carrier surfaces or from formate/bicarbonate decomposition. The latter groups have been observed spectroscopically on Al_2O_3 and TiO_2, but not on SiO_2 (*31*). The interaction of CO with the surface could proceed via oxygen anions, according to the reaction

$$CO + O_2^- \rightarrow CO_2 + V_{O^2} + 2e^-, \quad (1)$$

where V_{O^2} corresponds to an anionic vacancy and e^- to a quasi-free electron. Formate decomposition is not a probable source, since no H_2 was detected. Based on the quantity of CO_2 which was observed, the quantity of H_2 expected from formate decomposition would be within the detectability limits of the mass spectrometer. Thus, the most probable sources of CO_2 are

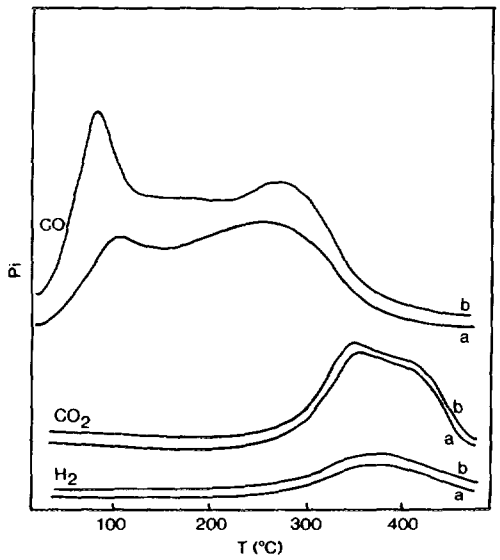

FIG. 2. TPD of CO from 0.5% Rh/SiO_2 catalyst following adsorption in the pulse (a) or continuous flow (b) modes at 25°C.

bicarbonate decomposition and/or oxidation of adsorbed CO.

TPD spectra of CO adsorbed on 0.5% Rh/SiO_2, either in the pulse mode or in the continuous flow mode for 15 min, are shown in Fig. 2. CO desorbs in the temperature range 40–350°C with two distinct peaks at 90–105°C and 260–270°C. CO_2 appears at temperatures higher than 300°C in the form of a broad peak. The appearance of CO_2 is accompanied by H_2 desorption. The H_2 peak is identical in shape and position to that of CO_2, which implies that both species have a common origin, which could be the reaction

$$CO(a) + H_2O \rightarrow CO_2 + H_2. \quad (2)$$

The effects of gaseous H_2O on CO TPD from Ru/Al_2O_3 catalysts have been demonstrated by Fujimoto *et al.* (*32*). In the present study, however, as indicated in the Experimental section, particular attention was paid to purify the gases used in these experiments so as to eliminate side reactions such as Eq. (2). Furthermore, the stoichiometry of Eq. (2) implies equal quanti-

ties of CO_2 and H_2 produced, which is not the case in the spectra of Fig. 2. The most probable origin of CO_2 and H_2 is the interaction of adsorbed CO on the Rh surface with surface hydroxyl groups of the carrier, according to

$$CO(a) + OH_{(S)} \rightarrow (COOH)_{(a)} \rightarrow CO_2 + \tfrac{1}{2}H_2. \quad (3)$$

Indeed, the quantity of H_2 observed in the TPD spectrum is approximately half that of CO_2.

As shown in Fig. 2, the quantity of CO_2 produced after pulse CO adsorption or adsorption under continuous CO flow for 15 min, is practically the same. This implies that CO_2 originates from strongly adsorbed CO on the Rh surface. The CO spectra, corresponding to the two different modes of adsorption (pulse and continuous flow), differ in the intensity of the first peak, whose maximum is at 105°C after pulse adsorption and 91°C after continuous flow adsorption. The shift is probably due to higher surface coverages achieved in the continuous flow mode of adsorption. A comparison of the two spectra indicates that the adsorption of CO is rapid and a few (2–3) pulses are sufficient to cover most of the Rh surface. Initially, the sites which correspond to strongly adsorbed CO are occupied while, at longer adsorption times the quantity of weakly adsorbed CO increases.

TPD spectra observed over the Rh/Al_2O_3 catalyst after CO adsorption in the pulse or the continuous flow mode are shown in Fig. 3. The CO spectrum consists of two main peaks at approximately 100 and 220–240°C. The CO_2 spectrum consists of a major peak at 330–350°C and of a smaller peak at 180°C. The high-temperature CO_2 peak is accompanied by an H_2 peak of the same shape and at the same position. Small quantities of CH_4 were also observed in the same temperature range, originating from the hydrogenation of CO. For the latter, the source of H_2 is likely that obtained from reaction (3). The CO_2 peak at 180°C which

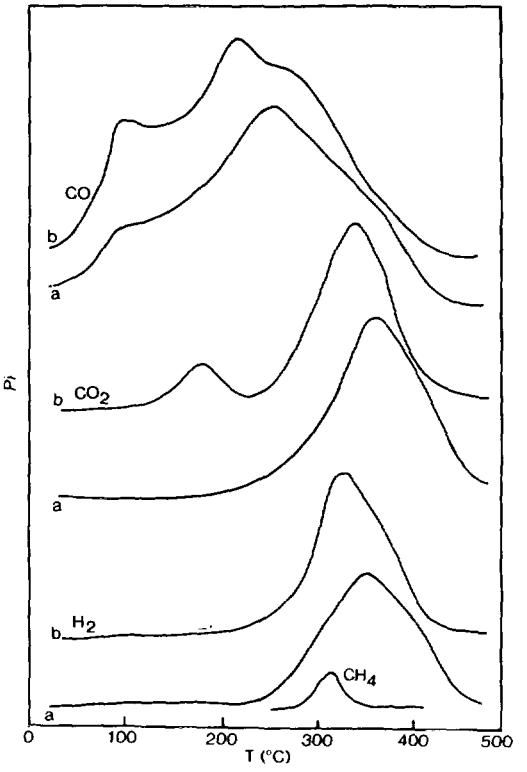

FIG. 3. TPD of CO from 0.5% Rh/Al_2O_3 catalyst following adsorption in the pulse (a) or continuous flow (b) modes at 25°C.

is not accompanied by H_2 desorption is attributed in its largest part to the decomposition of CO on the Rh surface (Boudouard reaction) (*16*, *18*). The quantity of weakly adsorbed CO which desorbs at low temperatures is enhanced in the continuous flow adsorption mode. The TPD spectra which were obtained over the Rh/Al_2O_3 catalyst are in good agreement with results obtained by other investigators (*2*, *16*, *17*).

In a different experiment, the Rh/Al_2O_3 catalyst was heated to 450°C under He flow and then cooled to room temperature under He flow prior to CO adsorption. The TPD spectra obtained are shown in Fig. 4, and they differ substantially from the spectra of Fig. 3. Heating of the catalyst under He results in partial dehydroxylation of the carrier surface. This gives rise to the ap-

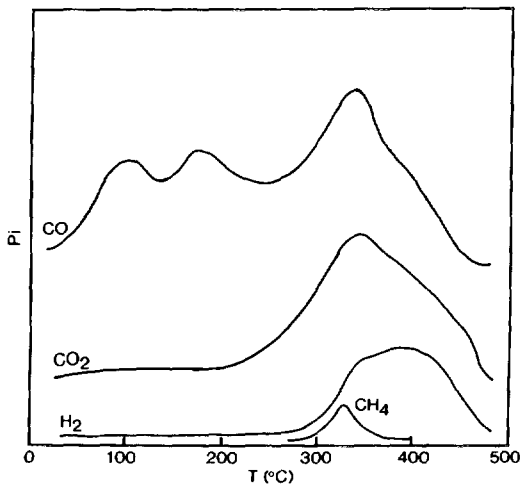

FIG. 4. TPD of CO from 0.5% Rh/Al_2O_3 catalyst, heated to 450°C under He flow, prior to CO adsorption at 25°C.

pearance of CO in the temperature range in which CO_2 appeared previously. Thus, CO_2 does indeed originate from strongly adsorbed CO which, as it desorbs interacts with surface hydroxyl groups of the carrier to produce CO_2 and H_2. The degree of this interaction and the quantity of CO_2 produced depends on the degree of hydroxylation of the surface. Thus the role of the metal in this process is to retain CO on the catalyst surface up to fairly high temperatures, where it is more likely to react with hydroxyl groups. Similar quantities of surface carbonates could probably be generated on metal-free carriers by CO exposure at the elevated temperatures encountered during TPD. An additional role of the metal could be the creation of surface hydroxyls from spillover hydrogen during the reduction step.

The TPD spectra obtained over the Rh/TiO_2 catalyst, after CO adsorption either in the pulse mode or in the continuous flow mode are shown in Fig. 5. The CO spectrum consists of a major peak at 145°C and two smaller peaks at 62 and 225–245°C. The CO_2 spectrum consists of three peaks at approximately 75, 150, and 270°C. The first CO peak originates from the carrier, since it was also observed in a similar experiment with unmetalized TiO_2. The peak at 270°C is accompanied by H_2 and CH_4 desorption indicating that this CO_2 originates in the interaction between CO and surface hydroxyl groups, as in the cases of Rh/SiO_2 and Rh/Al_2O_3. The 150°C peak is not accompanied by H_2 desorption, and it is at the same position with the main CO peak. This CO_2 must originate from the surface decomposition of CO according to

$$CO_{(a)} + CO_{(a)} \rightarrow C_{(a)} + CO_2. \qquad (4)$$

Two types of experiments were conducted in order to test the validity of reaction (4). In the first experiment, upon completion of the TPD run the catalyst was maintained at 400°C and the feed was switched from He (carrier gas) to 10% O_2 in He in order to titrate the carbon left on the surface during the TPD experiment. A sharp CO_2 peak was obtained and the quantity of CO_2 produced was found to be only 15% larger than the quantity of CO_2 which

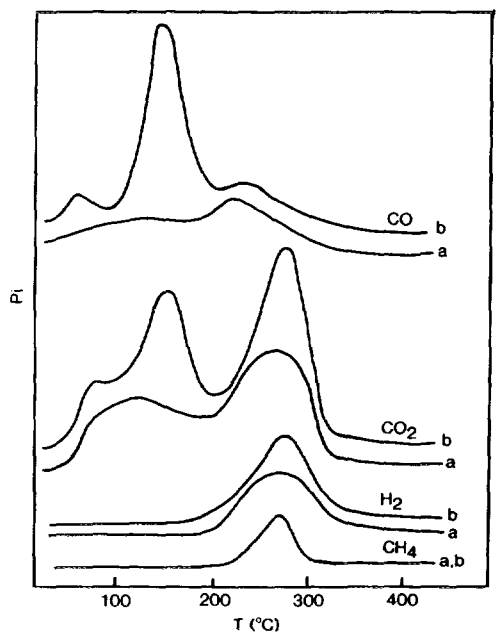

FIG. 5. TPD of CO from 0.5% Rh/TiO_2 catalyst, following adsorption in the pulse (a) or continuous flow (b) modes at 25°C.

corresponds to the peak at 150°C. This material balance satisfies the stoichiometry of reaction (4), strongly suggesting that the CO_2 peak at 150°C arises from the Boudouard reaction. The excess 15% CO_2 could originate from carbon associated with the higher temperature CO_2 peak. A second experiment was conducted in order to test whether removal of oxygen from the TiO_2 surface participates in CO_2 production, since it has been suggested by Paul *et al.* (*33*) that adsorbed CO reduces a portion of Ti^{+4} cations to Ti^{+3} and desorbs as CO_2. In this experiment the Rh/TiO_2 catalyst was exposed to $^{18}O_2$ at 600°C for 5 min, causing an appreciable isotope exchange in TiO_2. CO was subsequently adsorbed on this sample at 25°C and the TPD experiment was conducted in the usual manner. No CO_2 containing labeled oxygen was detected to desorb, indicating that surface lattice oxygen of TiO_2 does not participate in CO_2 production. The discrepancy between this result and that of Paul *et al.* (*33*) might be due to the fact that in the present study the catalysts are reduced under H_2 flow at 200°C prior to CO adsorption and initiation of TPD. This treatment might be expected to already reduce the portion of the TiO_2 surface around the Rh particles, thus prohibiting further reduction by CO.

It must also be noted that, as shown in Fig. 5, only a small fraction of the metallic surface is covered upon pulse adsorption, corresponding to the strongly adsorbed state, while the main CO peak at 145°C appears only after adsorption in the continuous flow mode. In contrast, in the Rh/SiO_2 and Rh/Al_2O_3 catalysts, pulse adsorption was sufficient to cover the largest fraction of the metallic surface.

The appearance of CO_2 and H_2 in the spectra has been attributed to the interaction of adsorbed CO with hydroxyl groups of the surface of the carrier. It is not clear whether this interaction takes place during CO adsorption or during CO desorption, as CO diffuses through the porous structure of the catalysts. The fact, however, that the quantity of CO_2 produced is not significantly affected by time of adsorption of CO (see Table 3) and the fact that very small quantities of CO_2 were detected to desorb from the unmetalized carriers lead to the conclusion that CO_2 originates from CO strongly adsorbed to the metallic surface. Thus, the interaction of CO with the surface hydroxyl groups occurs upon desorption of CO, as it diffuses through the particles. On the basis of this reasoning, it can be concluded that the position of the CO_2 peak reflects the strength of the adsorption of CO from which CO_2 originates.

A comparison of the TPD spectra obtained after CO adsorption on Rh/SiO_2, Al_2O_3, and TiO_2 (Figs. 3–5) reveals signifi-

TABLE 3

Peak Temperatures of TPD Spectra of CO from Rh/SiO_2, Al_2O_3, TiO_2, and Quantities of Species Desorbed

Catalyst Rh/	Adsorption mode	T_M (°C)		Quantities detected (cm³/g)		
		CO	CO_2	CO	CO_2	H_2
SiO_2	Pulse	104, 263	350	0.33	0.26	0.15
	Continuous	91, 270	340	0.45	0.26	0.14
Al_2O_3	Pulse	245	355	0.52	0.50	0.30
	Continuous	100, 210	180[a], 340	0.56	0.60	0.30
TiO_2	Pulse	230	120[a], 267	0.07	0.40	0.12
	Continuous	62, 145, 245	80[a], 150, 275	0.18	0.56	0.15

[a] Corresponds to desorption from the carrier.

cant differences, depending on the carrier employed to disperse the Rh crystallites. The desorption from the Rh/TiO_2 catalyst is completed at lower temperatures, as compared to that of Rh/SiO_2 and Rh/Al_2O_3. No CO decomposition was observed in the Rh/SiO_2 catalyst, in contrast to Rh/Al_2O_3 and Rh/TiO_2. CO decomposition is manifested in the CO_2 desorption peaks at 180 and 150°C, for Rh/Al_2O_3 and Rh/TiO_2, respectively. The activity of these catalysts towards CO decomposition seems to decrease in the order: $Rh/TiO_2 > Rh/Al_2O_3 \gg Rh/SiO_2$. It must also be emphasized that CO decomposition is not directly related to the strength of the CO adsorption bond. This is apparent in Fig. 2, which shows that strongly adsorbed CO on Rh/SiO_2 desorbs at approximately 270°C without decomposition (no CO_2 production) while weakly adsorbed CO on Rh/TiO_2 desorbs at 145°C (Fig. 5) decomposes to an appreciable extent. These results indicate that the nature of the carrier influences the state of CO adsorbed on Rh crystallites.

It has been observed (*11–14*) that CO does not decompose over Rh(111) or unsupported polycrystalline Rh surfaces. The same was observed in the present study for Rh/SiO_2. SiO_2 is generally considered to be one of the most inert carriers. However, when Rh is dispersed over TiO_2 its properties toward CO decomposition are altered. This phenomenon could be explained assuming that TiO_2 influences the morphology of the Rh crystallites. This explanation, however, is not very plausible since it has been shown that the crystallographic orientation of Rh surfaces does not influence the mode of CO adsorption (*15*). Another explanation could be that an electronic interaction develops at the $Rh–TiO_2$ interface, which influences the electronic structure of Rh and consequently the mode of CO adsorption. The effects of variation of electronic properties of TiO_2 carriers on CO dissociation and hydrogenation have been examined by Solymosi *et al.* (*34*), who demonstrated that variation of the electron density of TiO_2 influences the rate of these processes. This hypothesis, however, cannot explain why the decomposition of CO is not dependent on the strength of its adsorption on the metallic surface. The most plausible explanation is that new adsorption sites are created at the metal–support interface and the carrier participates or assists the process of CO decomposition or the reaction between produced carbon and surface oxygen species towards CO_2. This hypothesis can explain the observation that the decomposition of CO is not directly related to the strength of its adsorption, since the mechanism of the decomposition is viewed to be altered by participation of the TiO_2 carrier. Generally, the ease of dissociation is not related with the heat of adsorption of CO (*35, 36*) or to the coordination of CO to the surface. Two factors must be taken into consideration in order to examine the dissociation probability: (a) The intensity of backbonding from the metal to the CO molecule, and (b) the bond strength of the atomic components of the Rh surface. It should be also noted that there is a rather poor correlation between the extent of backbonding and the adsorption strength of CO (*36*), because the 5σ-metal bond as well as the metal work function play an important role. Thus, based on the above, the observation that the CO dissociation on Rh/TiO_2 corresponds to a weak form of adsorbed CO, is not at all strange. The concept of creation of new sites at the $Rh–TiO_2$ interface relates to factor (b) above if it is assumed that CO can be tilted with the O atom toward TiO_2, providing another easier pathway towards dissociation.

Peak temperatures of the TPD spectra of CO from Rh/SiO_2, Al_2O_3, TiO_2 are summarized in Table 3, along with the quantities of the species desorbed. Three major states of desorbing CO were detected, of which one desorbs as CO_2 accompanied by H_2 evolution. In the Rh/SiO_2 and Rh/Al_2O_3 catalysts, the weakly adsorbed CO exhibits peak temperatures in the range 90–100°C, while the strongly adsorbed CO appears at

263–270°C in Rh/SiO_2 and at 210–245°C in Rh/Al_2O_3. A weakening in the strength of adsorption of this adsorbed state over Rh/Al_2O_3 is therefore indicated. In both cases CO_2 appears in the range 340–355°C. A significant shift in the CO_2 peak toward lower temperatures (267–275°C) is observed over Rh/TiO_2. The CO spectrum over Rh/TiO_2 is significantly different than that over the other catalysts, and the peaks cannot be correlated with certainty.

The quantities of CO, CO_2 and H_2 detected to desorb are also reported in Table 3. CH_4 is not included since it accounts for less than 1% of CO desorbed. It is apparent that a major fraction of adsorbed CO desorbs as CO_2. In the Rh/Al_2O_3 and Rh/TiO_2 catalysts, CO_2 originates from (a) desorption from the carrier, approximately 8% in the case of Rh/Al_2O_3 and 5% in the case of Rh/TiO_2, (b) from CO decomposition, and (c) from reaction between CO and surface hydroxyl groups. In the case of Rh/SiO_2, CO_2 originates exclusively from reaction of CO with surface hydroxyls.

The quantity of CO desorbed can be utilized to estimate the CO/Rh ratio in the catalysts. Using the CO adsorbed after continuous flow adsorption, the CO/Rh ratio for the Rh/SiO_2 catalyst in approximately 0.7, for Rh/Al_2O_3 approximately 1.1, and for Rh/TiO_2, 0.6. The dispersion of the catalysts, as obtained by static equilibrium adsorption of H_2 is 1 for Rh/SiO_2 and Rh/Al_2O_3, and 0.7 for Rh/TiO_2.

(c) *Temperature-Programmed Reaction of Adsorbed CO with H_2*

The reactivity of CO adsorbed on Rh crystallites dispersed on SiO_2, Al_2O_3, or TiO_2 carriers was investigated by TPR of adsorbed CO with H_2. In these experiments, CO was adsorbed at room temperature under continuous flow for 15 min. The flow was subsequently switched to He for 3 min to purge the gas phase of the reactor from CO and to clean the lines. The flow was then switched to H_2 and temperature programming was initiated at a rate of 23°C/min. The main products of reaction of H_2 with adsorbed CO are CH_4 and H_2O. In addition to these products, in the case of Rh/SiO_2 catalyst, CO was also observed to desorb unreacted with a peak at approximately 90°C which corresponds to the peak at 91–105°C of the TPD spectrum of the same catalyst. In the TPR spectra of the other two catalysts, no CO was observed to desorb in measurable quantities.

The CH_4 TPR spectra of the three catalysts investigated are shown in Fig. 6. Over the Rh/SiO_2 catalyst, CH_4 appears at approximately 80°C, while the peak temperature is at 230°C and CH_4 production is completed at 270°C. Over the Rh/Al_2O_3 catalyst, CH_4 production is initiated at approximately 100°C, while the peak maximum is at 200°C and the reaction is completed at approximately 260°C. Over the Rh/TiO_2 catalyst, CH_4 appears at approximately 65°C, while peak maximum is at 120°C and the reaction is completed at 180°C. It is apparent that the shape and the position of the CH_4 peak in the temperature scale are a strong function of the carrier

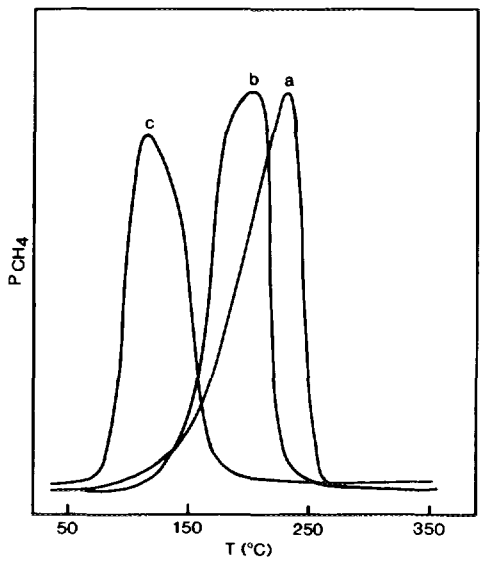

FIG. 6. TPR of adsorbed CO under H_2 flow over 0.5% Rh/SiO_2 (a), 0.5% Rh/Al_2O_3 (b), and 0.5% Rh/TiO_2 (c) catalysts. CO was adsorbed at 25°C with the continuous flow mode.

employed to disperse the Rh crystallites. The activity for hydrogenation of the adsorbed CO follows the order: $Rh/TiO_2 \gg Rh/Al_2O_3 > Rh/SiO_2$. These results are in good agreement with the results of Fujimoto *et al.* (*32*), who observed a single methane peak over Rh/SiO_2 at 222°C, and at 147°C over Rh/Al_2O_3. Their heating rate, however, was significantly lower than that of the present study (7 vs 23°C/min). It has been established that high heating rates shift the peak temperatures towards higher values (*28, 29*). Efstathiou (*16*) also observed a single peak over Rh/Al_2O_3 at 220°C, with a heating rate of 30°C/min.

Recently, Falconer and co-workers conducted extensive TPR studies of CO adsorbed on Pd (*37*), Pt (*38*) and Ni (*39–41*) dispersed on various carriers. They demonstrated the existence of two distinct CH_4 formation pathways, one involving the direct hydrogenation of CO adsorbed on the metal and one involving conversion of metal-adsorbed CO to support-bound methoxy which is subsequently hydrogenated to CH_4. The second path was found to depend on the support and to be important for Al_2O_3 and TiO_2 supported catalysts but not for SiO_2 supported catalysts. In Ni/Al_2O_3 and Ni/TiO_2 catalysts, for example, two CH_4 peaks were observed; the low-temperature one was attributed to hydrogenation of CO bound to Ni and the high-temperature one to hydrogenation of the CH_3O-species.

The single TPR peak observed in the present study, in most probability, is due to direct hydrogenation of metal-bound CO for the following reasons: (a) the conditions of the present TPR experiments were the least favorable for CH_3O formation, since CO adsorption was conducted at low temperature and the reactor was cleaned with He flow prior to initiation of temperature programming under H_2 flow. Falconer and co-workers (*39–41*) observed an extremely weak $CH_3O \rightarrow CH_4$ peak when CO adsorption was conducted at room temperature on Ni/TiO_2. (b) It was demonstrated that CH_3O formation does not take place on SiO_2-supported catalysts. Therefore, the peak observed in the present study over the Rh/SiO_2 catalyst must arise from hydrogenation of CO bound to Rh. (c) the CH_4 peak over Rh/TiO_2 was observed at 120°C, while Falconer and co-workers observed $CH_3O \rightarrow CH_4$ peaks over Ni/TiO_2 at 251°C, and over Pt/TiO_2 at approximately 230°C, with a heating rate of 60°C/min, which shifted to 190°C under a heating rate of 6°C/min. Over Rh/Al_2O_3, in the present study, the CH_4 peak was observed at 200°C while Falconer and co-workers observed the $CH_3O \rightarrow CH_4$ peaks at 272°C over Pd/Al_2O_3 and at 267°C over Ni/Al_2O_3. Thus, the peak temperatures observed in the present study are significantly lower than those assigned to the $CH_3O \rightarrow CH_4$ process, even taking into account the different heating rates employed. It should be noted that the energetics of this CH_4 formation process were found to be sensitive to the carrier employed and not to the particular metal.

(*d*) *Steady-State CO Hydrogenation*

The influence of the carrier on kinetic parameters in CO hydrogenation was also investigated employing the Rh/SiO_2, Al_2O_3, and TiO_2 catalysts. Kinetic results in terms of turnover frequencies of CO consumption, methanation and water–gas shift reactions are summarized in Table 4, along with the activation energies of the two reaction routes. The kinetic experiments were conducted at 210°C with a feed H_2/CO ratio of 3. Activation energies were determined in the temperature range of 170–250°C. The Rh/TiO_2 catalyst is 15–20 times more active than the Rh/SiO_2 and Rh/Al_2O_3 catalysts, which exhibit comparable activity at 210°C. The apparent activation energies are in the range 25–30 kcal/mol. The highest activation energy is exhibited by the Rh/SiO_2 catalyst, for both reaction paths. The apparent activation energies observed over Rh/TiO_2 are approximately 5 kcal/mol lower than those observed over Rh/SiO_2. The product distribution obtained over the various cata-

TABLE 4

Steady-State Kinetic Results of CO Hydrogenation over Rh/SiO_2, Al_2O_3, and TiO_2 Catalysts (T = 210°C, H_2/CO = 3)

Catalyst Rh/	N_{CH_4}	N_{CO_2} ($s^{-1} \times 10^3$)	N_{CO}	E_{CH_4}	E_{CO} (kcal/mol)
SiO_2	0.06	0	0.07	30.5	29.7
Al_2O_3	0.07	0.02	0.15	27.0	24.6
TiO_2	1.2	0.2	2.5	26.0	25.0

lysts under the same reaction conditions is shown in Table 5. The Rh/SiO_2 catalyst exhibits the lowest selectivity towards higher hydrocarbons while the Rh/TiO_2 the highest. Furthermore, essentially no CO_2 was observed over the Rh/SiO_2 catalyst, in contrast to the other catalysts, as indicated in Table 4. The steady-state activity and selectivity results are in good agreement with results reported by other investigators (*18–20, 42–44*).

The TPD and TPR results discussed in previous sections can assist in understanding the steady-state behavior of the catalysts under CO hydrogenation conditions. The H_2 TPR of adsorbed CO reveal that the activity of adsorbed CO toward hydrogenation to CH_4 is in good agreement to the activity observed under steady-state conditions. Correlating the activity of adsorbed CO to its adsorption characteristics, as revealed from TPD experiments, it can be seen that activity increases with the ease of dissociation of the adsorbed CO.

TABLE 5

Product Distribution Observed over the Rh/SiO_2, Al_2O_3, and TiO_2 Catalysts under CO Hydrogenation at 210°C

Catalyst Rh/	Selectivity (mol%)								
	CH_4	C_2H_4	C_2H_6	C_3H_6	C_3H_8	C_4	C_5	C_6	C_7
SiO_2	95.2	<0.1	2.7	0.3	1.0	0.5	0.2	—	—
Al_2O_3	79.2	0.9	5.7	5.9	2.0	3.2	1.5	0.8	—
TiO_2	80.5	0.8	0.8	5.6	0.3	6.1	2.4	1.6	1.1

The following mechanistic picture can be visualized, based on these observations: A basic reaction step is the dissociation of adsorbed CO toward atomic C. Rh/SiO_2, on which CO dissociation is negligible, is the least active catalyst, exhibiting the highest activation energy which reflects the high activation barrier for dissociation and the large heat of adsorption of CO. Selectivity toward CH_4, exhibited by this catalyst, is high because of low surface coverage of active C. Rh/Al_2O_3 and especially Rh/TiO_2 exhibit higher activity due to enhanced CO dissociation. Activation energies are also lower over these catalysts, corresponding to lower activation barriers for CO dissociation.

The nature of the Rh–support interaction which influences the adsorptive and catalytic behavior of Rh is not well understood. Phenomena related to SMSI, such as decoration of Rh particles with reduced TiO_x species cannot have taken place in the present study since the catalyst was never exposed to a temperature higher than 250°C. While the TiO_2 surface can be reduced from spillover atomic hydrogen adsorbed on Rh, the migration of TiO_x species is an activated process and is probably negligible at these low temperatures. Furthermore, the Rh/TiO_2 catalyst did not exhibit any anomalously low H_2 or CO chemisorption capacity, a feature commonly found in SMSI catalysts. The possibility of long-range electronic interactions, affecting the electronic structure of the Rh surface (*34*) must also be considered. TiO_2 is an n-type semiconductor and its n-conductivity increases in reducing conditions. The work function of reduced TiO_2 can be lower than that of Rh, leading to charge transfer from the semiconductor to the metal. However, undoped TiO_2 has a small free electron concentration and the quantity of charge transferred cannot be significant enough to alter the electronic properties of the Rh crystallites. On the other hand, the possibility of localized effects at the periphery of the Rh crystallites appears rather strong. Among

the carriers employed in the present investigation, TiO_2 in the only reducible oxide. Thus, the creation of new active sites at the metal–support interface or a direct interaction between Rh atoms at the periphery with reduced TiO_2 species are highly probable. This could be related to the formation of methoxy species at the periphery of the Rh particles, which then decompose to CH_4, as illustrated by Falconer and coworkers (*37–41*). Although this route was not detected on the present catalysts under TPR conditions, it could play an important role under steady-state hydrogenation conditions since both CO and H_2 are present on the catalyst surface, at elevated temperatures.

SUMMARY AND CONCLUSIONS

The interaction of H_2 and CO with Rh crystallites dispersed on SiO_2, Al_2O_3, and TiO_2 carriers was investigated with TPD and TPR techniques. H_2 TPD spectra consist, in general, of two peaks at 70–100°C and 160–200°C, which can be attributed to two different states of adsorbed H_2. The high-temperature peak which corresponds to strongly adsorbed H_2 increases significantly when adsorption takes place at higher temperatures. The carrier used to disperse the metal influences the relative intensity of the two peaks but not their position in the temperature scale. Comparison of the spectra obtained in this work with spectra obtained over Rh(111) surfaces implies that the carrier and possibly the Rh crystallite size influence significantly the mode of H_2 adsorption. Peak maxima were observed to shift to higher temperatures with increasing temperature of adsorption. Furthermore, the quantity of H_2 desorbed from Rh/TiO_2 was also found to increase with increasing temperature of adsorption. This has been attributed to activated adsorption, and/or increased strength of the adsorption bond and subsequently reduced H_2 desorption prior to initiation of the TPD experiments.

CO TPD spectra were found to be significantly affected by the nature of the support of the Rh crystallites. Significant CO dissociation was observed over Rh/TiO_2 and to a smaller extent on Rh/Al_2O_3 but not on Rh/SiO_2. The dissociation of CO does not seem to be directly related to the strength of the Rh–CO adsorption bond. It is proposed that the dissociation is at least partially assisted by sites at the metal–support interface. In addition to the CO dissociation process, the appearance of CO_2 has been attributed to interaction of CO with surface hydroxyl groups upon desorption of strongly adsorbed CO. A significant shift of peak temperatures towards lower values was also observed over Rh/TiO_2.

The reactivity of adsorbed CO towards hydrogenation was investigated by TPR experiments and was found to be significantly affected by the nature of the carrier. Reactivity was found to decrease in the order: $Rh/TiO_2 \gg Rh/Al_2O_3 > Rh/SiO_2$. The same order was observed in CO dissociation, which might imply that CO dissociation is an intermediate step in the process of CO hydrogenation. Furthermore, the same order of reactivity, with respect to the carrier employed to disperse the Rh crystallites, was observed in steady-state CO hydrogenation experiments.

REFERENCES

1. Vannice, M. A., and Twu, C. C., *J. Catal.* **82,** 213 (1983).
2. Erdöhelyi, A., and Solymosi, F., *J. Catal.* **84,** 446 (1983).
3. Mori, Y., Mori, T., Miyamoto, A., Takamashi, N., Hattori, T., and Murakami, Y., *J. Phys. Chem.* **93,** 2039 (1989).
4. Inoue, T., Iizuka, T., and Tanabe, K., *Appl. Catal.* **46,** 1 (1989).
5. Boccuzi, F., Chiorino, A., Chiotti, G., Pinna, F., Strukul, G., and Tessori, R., *J. Catal.* **126,** 381 (1990).
6. Yates, J. T., Thiel, P. A., and Weinberg, W. H., *Surf. Sci.* **84,** 427 (1979).
7. Efstathiou, A. M., and Bennett, C. O., *J. Catal.* **124,** 116 (1990).
8. Bertucco, A., and Bennett, C. O., *Appl. Catal.* **35,** 329 (1987).

9. Apple, T. M., Gajardo, P., and Dybowski, C., *J. Catal.* **68,** 103 (1981).
10. Stockwell, D. M., Bertucco, A., Coulson, G. W., and Bennett, C. O., *J. Catal.* **113,** 317 (1988).
11. Yates, J. T., Williams, E. D., and Weinberg, W. H., *Surf. Sci.* **91,** 562 (1980).
12. Thiel, P. A., Williams, E. D., Yates, J. T., and Weinberg, W. H., *Surf. Sci.* **84,** 54 (1979).
13. Mate, C. M., and Somorjai, G. A., *Surf. Sci.* **160,** 542 (1985).
14. Bertel, E., Rosina, G., and Netzer, F. R., *Surf. Sci.* **172,** L515 (1986).
15. Altman, E. I., and Gorte, R. J., *Surf. Sci.* **195,** 392 (1988).
16. Efstathiou, A. M., Ph.D. dissertation, University of Connecticut, 1989.
17. Oh, S. H., and Eickel, C. C., *J. Catal.* **112,** 543 (1988).
18. Efstathiou, A. M., and Bennett, C. O., *J. Catal.* **120,** 118 (1989); 120, 137 (1989).
19. Katzer, J. R., Sleight, A. W., Gajardo, P., Michel, J. B., Gleason, E. F., and McMillan, S., *Faraday Discuss. Chem. Soc.* **72,** 121 (1982).
20. Solymosi, F., Tombacz, I., and Kocsis, M., *J. Catal.* **75,** 78 (1982).
21. Vant Blik, H. F. J., Vis, J. C., Huizinga, T., Prins, R., *Appl. Catal.* **19,** 405 (1985).
22. Taniguchi, S., Mori, T., Mori, Y., Hattosi, T., and Murakami, Y., *J. Catal.* **116,** 108 (1989).
23. Levin, M. E., Salmeron, M., Bell, A. T., and Somorjai, G. A., *J. Catal.* **106,** 401 (1987).
24. Braunschweig, E. J., Logan, A. D., Datye, A. K., and Smith, D. J., *J. Catal.* **118,** 227 (1989).
25. Demmin, R. A., and Gorte, R. J., *J. Catal.* **90,** 32 (1984).
26. Rieck, J. S., and Bell, A. T., *J. Catal.* **85,** 143 (1984).
27. Ioannides, T., and Verykios, X. E., *J. Catal.* **120,** 157 (1989).
28. Leary, K. J., Michaels, J. N., and Stacy, A. M., *Langmuir* **4,** 1251 (1988).
29. Lee, P. I., and Schwartz, J. A., *J. Catal.* **13,** 272 (1982).
30. Guczi, L., *in* "New Trends in CO Activation" (L. Guczi, Ed.), Studies in Surface Science and Catalysis, Vol. 64, p. 351. Elsevier, Amsterdam, 1991.
31. Rethwisch, D. G., and Dumesic, J. A., *Langmuir* **2,** 73 (1986).
32. Fujimoto, K., Kameyama, M., and Kubugi, J., *J. Catal.* **61,** 7 (1980).
33. Paul, J., Cameron, S. D., Dwyer, D. J., and Hoffmann, F. M., *Surf. Sci.* **177,** 121 (1986).
34. Solymosi, F., Tombacz, I., Koszta, J., *J. Catal.* **95,** 578 (1985).
35. van Santen, R. A., and de Koster, A., *in* "New Trends in CO Activation" (L. Guczi, Ed.), Studies in Surface Science and Catalysis, Elsevier, Amsterdam, 1991.
36. Kiskinova, M., *in* "New Trends in CO Activation" (L. Guczi, Ed.), Studies in Surface Science and Catalysis, Vol. 64, p. 37. Elsevier, Amsterdam, 1991.
37. Hsiao, E. C., and Falconer, J. L., *J. Catal.* **132,** 145 (1991).
38. Mao, T. F., and Falconer, J. L., *J. Catal.* **123,** 443 (1990).
39. Sen, B., and Falconer, J. L., *J. Catal.* **122,** 68 (1990); **125,** 35 (1990).
40. Sen, B., Falconer, J. L., Mao, T. F., Yu, M., and Flesner, R. L., *J. Catal.* **126,** 465 (1990).
41. Chen, B., Falconer, J. L., and Chang, L., *J. Catal.* **127,** 732 (1991).
42. Jackson, S. D., Brandreth, B. J., and Winstanley, D., *J. Chem. Soc. Faraday Trans. I* **84,** 1741 (1988).
43. Duprez, D., Barrault, J., and Geron, C., *Appl. Catal.* **37,** 105 (1988).
44. Vannice, M. A., *J. Catal.* **74,** 199 (1982).